Effect of antiphase boundaries on the electronic structure and bonding character of intermetallic systems: NiAl

T. Hong
Department of Physics and Astronomy, Northwestern University, Evanston, Illinois 60208-3112

A. J. Freeman
Department of Physics and Astronomy, Northwestern University, Evanston, Illinois 60208-3112 and Argonne National Laboratory, Argonne, Illinois 60349

(Received 13 August 1990)

The possible origin of the high degree of brittleness, i.e., low ductility, of the NiAl-based alloys in the $B2$ structure is investigated by all-electron self-consistent total-energy linear-muffin-tin-orbital calculations. Using a supercell approach (with up to 20 atoms/unit cell), the energetics of the two simplest antiphase boundaries (APB's) for NiAl in the $B2$ structure—namely the $\frac{1}{2}\langle 111\rangle$ on $\{110\}$ and $\frac{1}{2}\langle 111\rangle$ on $\{112\}$—are calculated assuming no relaxation at the interface. We find APB energies of the order of 800 mJ/m^2 for both cases. Since the calculated APB energies are very high, $\langle 111\rangle$ slip is unlikely to occur—as suggested experimentally and by some phenomenological theories. By substituting Ni or Al with V, Cr, or Mn at the APB interfacial planes, remarkably decreased APB energies are obtained. These theoretical results on simplified model systems may suggest a way to decrease the APB energy in order to eliminate one of the possible reasons for the brittleness at ambient temperatures.

I. INTRODUCTION

The $B2$ compound NiAl, used as high-temperature oxidation-resistant coatings for some time,[1,2] has been studied intensively in recent years due to its potential for aerospace applications at high temperatures.[3–7] It has a low density (5.9 g cm^{-3}, compared to 8.5 g cm^{-3} for typical Ni-based superalloys[8]), a high melting point (1638 °C), a high modulus (189 GPa), and a wide stability range in atomic composition. It is also very stable [with a formation energy of 1405 kcal/g atom (Ref. 9)] and is strongly ordered up to the melting temperature. The major obstacle preventing it from practical use, however, is its intrinsic brittleness at ambient temperatures.

To understand the deformation mechanism, many experimental studies have been performed since the mid 1960s. Despite the repeated reports[10] of slip other than $\langle 100\rangle$, it is generally believed that the major deformation mode in $B2$ NiAl is $\langle 100\rangle$ slip,[10–14] especially at low temperatures. As $\langle 100\rangle$ slip can only provide three independent slip systems,[11,15] the five independent slip systems requirement for a polycrystal to be ductile (the von Mises criterion[16]) is not met. Therefore, polycrystalline NiAl is deformed by a brittle intergranular fracture at room temperature.[17] The generation of limited ductility through special technological means such as casting and extrusion,[18,19] grain refinement,[20] rapid solidification,[21–23] partial recrystallization,[3,24] and a thin-film approach[25] have been reported. For a variety of reasons, these efforts, however, are not considered to be totally successful.[1]

Since $\langle 111\rangle$ slip is prevalent in bcc metals and some other $B2$ intermetallic compounds,[3,26–28] and since the von Mises requirement would obviously be fulfilled if $\langle 111\rangle$ slip were to operate, some efforts have been made toward promoting $\langle 111\rangle$ slip in $B2$ NiAl.[14,29–31] Miracle *et al.*[14] found that the major deformation mode in $B2$ NiAl with ternary additions of Cr and Mn is indeed $\langle 111\rangle$ slip at low temperatures, although they revert to $\langle 100\rangle$ slip at high temperatures. Our calculations[29] and the closely related experimental studies of Darolia *et al.*[30,31] were all done following the same expectation.

As a low antiphase boundary (APB) energy might indicate easy formation of slip in the corresponding direction,[3] in this paper we further analyze the results from our APB energy calculations and the effects of the APB's on the bonding character and electronic structure of the $B2$ NiAl and its modified systems. Consequently, the possibility of promoting $\langle 111\rangle$ slip in $B2$ NiAl by the reduction of APB energies through alloying additions is discussed.

II. METHODOLOGY

A number of electronic-structure calculations have been reported over the past 20 years[32–39] for $B2$ NiAl which include a wide variety of methods such as non-self-consistent augmented plane wave (APW),[32] a fast version of the self-consistent Korringa-Kohn-Rostoker (KKR),[33] self-consistent cluster discrete variation (DVM),[34,39] non-self-consistent hybrid nearly-free-electron tight binding (HNFETB),[35] self-consistent augmented spherical wave (ASW),[36,39] and self-consistent APW with HNFETB (Ref. 37) and tight binding.[38] However, all these calculations concentrated on the electronic

properties without addressing the question of the brittleness.

We have applied the first-principles linear-muffin-tin-orbital (LMTO) method[40] including the combined correction terms to calculate the APB energies for the two most probable APB's, namely, $\frac{1}{2}\langle 111\rangle$ on $\{110\}$ and $\frac{1}{2}\langle 111\rangle$ on $\{112\}$ for pure $B2$ NiAl and $\frac{1}{2}\langle 111\rangle$ on $\{110\}$ for $B2$ NiAl with ternary additions of Mn, Cr, or V substituting for either Ni or Al atoms. For simplicity, we considered four smallest APB cells with four, six, eight, and ten layers of (100) and (112) planes, corresponding to unit cells with 8, 12, 16, and 20 atoms, respectively.

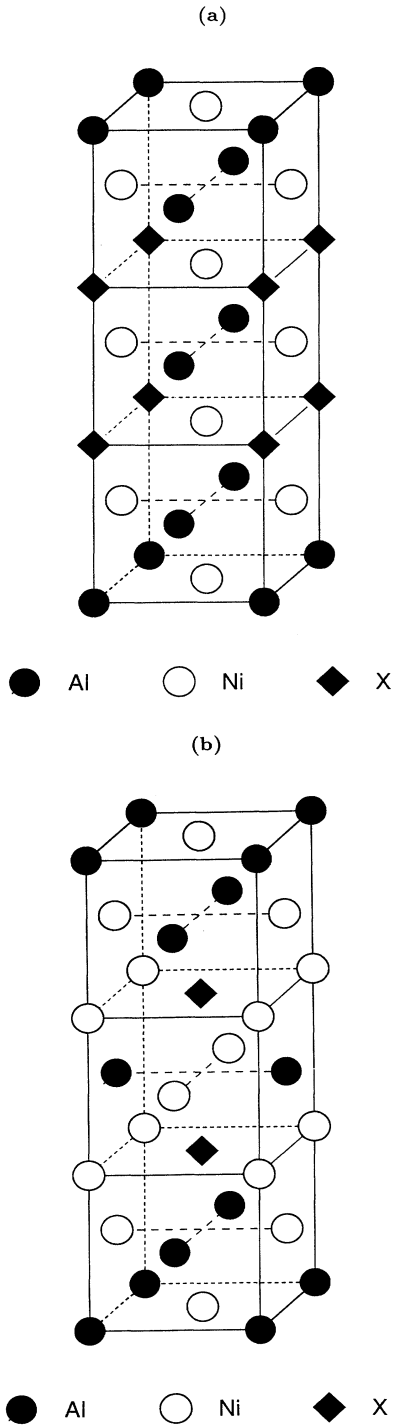

FIG. 1. Structure of $Ni_6Al_4X_2$ for (a) $B2$ and (b) $B2$ with APB's.

Schematically, the introduction of APB's can be represented in terms of the changes in the stacking sequence. We take the $\frac{1}{2}\langle 111\rangle$ on $\{110\}$ as an example. The stacking sequence in $B2$ NiAl along the $\langle 110\rangle$ direction can be denoted by AB. If A' and B' represent the corresponding A and B layers displaced by $\frac{1}{2}\langle 111\rangle$ on the (110) plane, the stacking sequence of four-, six-, eight-, and ten-layer $\frac{1}{2}\langle 111\rangle$ on $\{110\}$ APB's can be abbreviated as $ABA'B$, $ABA'B'A'B$, $ABAB'A'B'AB$, and $ABAB'A'B'A'B'AB$, respectively. An APB is created between two successive layers, of which only one is a primed layer. Thus, the number of APB's in the supercells is 2 regardless of the number of layers in the unit cells. However, as the number of layers between the two APB's increases, the interaction between neighboring APB's is expected to become less important—as will be shown more clearly in later sections.

In these model calculations, atomic relaxation at the APB interface is neglected. In the calculations for systems with ternary additions, we assume the ternary atoms to lie in the APB planes; this is much too simplified a model as it tends to exaggerate the effect of the ternary additions on the APB's by totally replacing one of the major constituents (i.e., Ni or Al) on the APB planes. One set of the unit cells actually used in the calculations ($\frac{1}{2}\langle 111\rangle$ on $\{110\}$ with six layers) is shown in Figs. 1(a) ($B2$ cell) and 1(b) ($B2$ cell with APB's). Thus, if the sites for ternary additions are actually occupied by Ni or Al to make the unit cell stoichiometric NiAl, the supercell represents the pure NiAl case. As earlier calculations have given satisfactory results for compounds $TiAl_3$ (Ref. 41) and Ti_3Al (Ref. 42), angular momentum components up to $l=2$ for Ni and Al, as well as for the ternary atoms, are included. The lattice constants used correspond to the observed value of $B2$ NiAl (2.886 Å).[43] The self-consistent iterations are carried out until the relative difference between input and output charge as well as potential reaches 10^{-3}.

III. RESULTS FOR PURE NiAl

A. APB energies

To avoid possible systematic error contributions to the calculated APB energies by using unit cells of different symmetry and size, we performed calculations for $B2$ NiAl both with the primitive unit cell and with supercells of the same size as are used in the corresponding APB calculations. After extrapolating the results to an infinite number of k points in the Brillouin zone, the results from the primitive and supercell calculations for $B2$ NiAl are identical within the precision of the method [~ 1 mRy (Ref. 40)] and give us confidence in the precision of the calculated APB energies.

By comparing the total energy from the supercells with

and without APB's, we found the APB energies to be around 800 mJ/m^2 for all the different layer calculations (cf., Table I). As the distance between two consecutive APB's is increased, the APB energies decrease gradually, as expected. The difference between the values from eight- and ten-layer calculations is very small, thus showing signs of convergence. This suggests that the interaction between two APB's is significant only within a certain range, after which two consecutive APB's can be considered as nearly independent, and hence the APB energy becomes independent of the number of layers. From our calculations, the values obtained for ten layers appear to be very good approximations for the extrapolated APB energies.

These calculated APB energies are extremely high, especially when compared with the result for APB's in Ni_3Al [150 mJ/m^2 for (100) APB (Ref. 44)]. They are between the two crude estimates of Potter[28] (223 mJ/m^2), which took into account only the first nearest neighbors and employed the Bragg-Williams approximation, and of Girifalco and Alonso[45] (2073 mJ/m^2), which used the Cragg-Fletcher assumption. Recently, Rudy and Sauthoff[46] simply mentioned the APB energy of 400 mJ/m^2 for $B2$ NiAl from an unpublished work. Unfortunately, they did not give any details. Since our calculated APB energies for $\frac{1}{2}\langle 111\rangle\{110\}$ and $\frac{1}{2}\langle 111\rangle\{112\}$ are comparable, we concentrate on the $\frac{1}{2}\langle 111\rangle$ on $\{110\}$-type APB in the following analysis.

As we will discuss more fully later, the creation of APB's in $B2$ NiAl introduces changes in the first nearest neighbors, which may be used to explain the high APB energies of $B2$ NiAl. The first- and second-nearest-neighbor configurations for six-layer-cell NiAl (with and without APB's) are listed in Table II. It is clearly seen that a quarter of the first nearest neighbors (two out of eight) for the atoms on the APB interfacial planes have been changed, while in contrast no first nearest neighbor is changed for the creation of (001) APB's in Ni_3Al which gave the considerably lower APB energy mentioned above.

Recently, Fu[47] reported calculations of APB energies in Al_3Ti and Al_3Sc, in which no first-nearest-neighbor change is involved, as in Ni_3Al. APB energies of the order of 400 mJ/m^2 were obtained. Thus, our calculated APB energies for $B2$ NiAl are very high when compared with these well-studied intermetallic compounds, implying stronger bonding which, in turn, is indicated by a high melting temperature. To our knowledge, no observation of APB's in $B2$ NiAl has been reported—which is consistent with large APB energies.

TABLE I. APB energies for $B2$ NiAl.

Number of layers in supercell	APB energies (mJ/m^{-2}) $\frac{1}{2}\langle 111\rangle\{110\}$	$\frac{1}{2}\langle 111\rangle\{112\}$
4	1130	1050
6	1000	950
8	880	890
10	880	885

TABLE II. The first- and second-nearest-neighbor (NN) configurations for $B2$ NiAl with and without APB's (for the six-layer APB cell which has the stacking sequence $ABA'B'A'BA$). Al(1)–Al(4) [Ni(1)–Ni(4)] represent the Al (Ni) atoms on the layers A, B, A', and B' of the unit cell, respectively.

	1st NN		2nd NN	
	same	other	same	other
		$B2$		
(all) Al, Ni	0	8	6	0
		$B2$ with APB's		
Al(1), Ni(1)	0	8	6	0
Al(2), Ni(2)	2	6	4	2
Al(3), Ni(3)	2	6	4	2
Al(4), Ni(4)	0	8	6	0

An earlier study by the embedded-atom method (EAM) showed that the change of APB energies due to relaxation could be about 20% for the cases where no first-nearest-neighbor change is involved.[48] We estimate that an even greater effect could possibly happen in the NiAl because of changes in the first nearest neighbors. Nonetheless, the APB energies would still be very high after a hypothetical but large reduction of 50%. Thus, the values from our calculations should be qualitatively correct.

B. Comparison of densities of states

The calculated density of states (DOS) for $B2$ NiAl is found to be independent of the symmetry and size of the supercells used in our calculations, as is the case with other features discussed above, and also in generally good agreement with other theoretical and experimental studies.[32–39,49–51] For comparison, the total DOS of $B2$ NiAl and that with APB's (six-layer case) is plotted in Figs. 2(a) and 2(b), and the partial density of states at each site for the two cases is plotted in Figs. 3(a) and 3(b). The "pseudogap"[38] or "quasigap"[39] near the Fermi energy (on the low-energy side) is clearly seen in the plots from our $B2$ calculation, showing good agreement with earlier work. With inclusion of the APB's, however, this gap disappears as can be seen in Fig. 2(b).

By comparing the partial DOS of the $B2$ and $B2$ with APB cells at individual sites, the major source for the changes is found immediately. The d components of the partial DOS at Ni(1) and Ni(4) sites (cf., the definition in Table II) are only slightly changed. On the other hand, those at Ni(2) and Ni(3) sites for the $B2$ with APB's case are modified significantly from the $B2$ case. At all sites, the gap is not as obvious as in the $B2$ case, or rather we might say that the gap just disappears. The d bands at the Ni(2) and Ni(3) sites become more dispersed and the bandwidth is increased, especially toward higher energy.

Being interested in the electronic and magnetic properties of $B2$ NiAl, Ellis *et al.*[34] and Sarma *et al.*[39] performed simple model cluster calculations which included only a center Ni (Al) and its eight nearest neighbors.

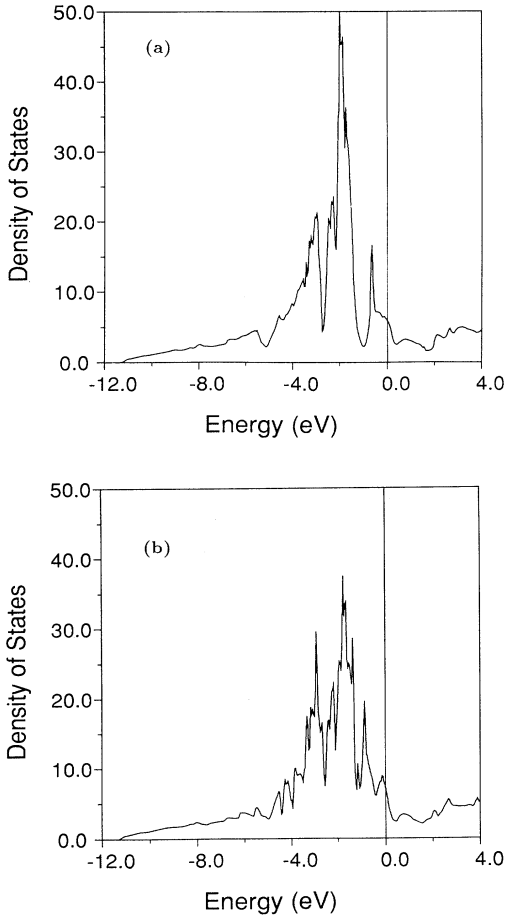

FIG. 2. Total density of states of NiAl for (a) $B2$ NiAl and (b) $B2$ NiAl with APB's (in states/eV unit cell).

Since major features of their DOS plots resembled those from bulk NiAl calculations, the interaction between the nearest-neighbor Ni and Al atoms appears to be predominantly important in NiAl. From the Ni d bandwidth in $B2$ NiAl obtained in an x-ray photoemission spectroscopy (XPS) study, Fuggle *et al.*[50] argued that Ni d states interact strongly with Al states and that the electronic behavior of NiAl can be better described by the concept of "mixing" (hybridization) than that of charge transfer. Hackenbracht *et al.*[36] even separated the contributions to bonding from individual sites and angular momentum components by decomposing the virial electronic pressure from their ASW calculations. Their results showed the importance of interactions between Ni d and Al p components.

Except for the tight-binding calculations of Colinet[38] in which the Fermi energy sits at a different position, our calculations and all the remaining earlier theoretical studies locate the Fermi energy at about 0.8 eV above a small distinctive peak identified by Moruzzi *et al.*[33] as due to the bands near the zone face defined by Γ, X, and R. The density-of-states results from more sophisticated methods (such as APW, KKR, ASW, and LMTO) resembled each other even in fine features, thus unambigiously indicating the agreement of modern first-principles band methods.

In the hypothetical NiNi calculations (with Al replaced by Ni in the NiAl lattice) done by Moruzzi *et al.*,[33] the major part of the Ni d bands are found just below E_F with a bandwidth that is one-third wider than that of $B2$ NiAl. In this case, each Ni atom has eight first-nearest-neighbor Ni atoms and the interaction be-

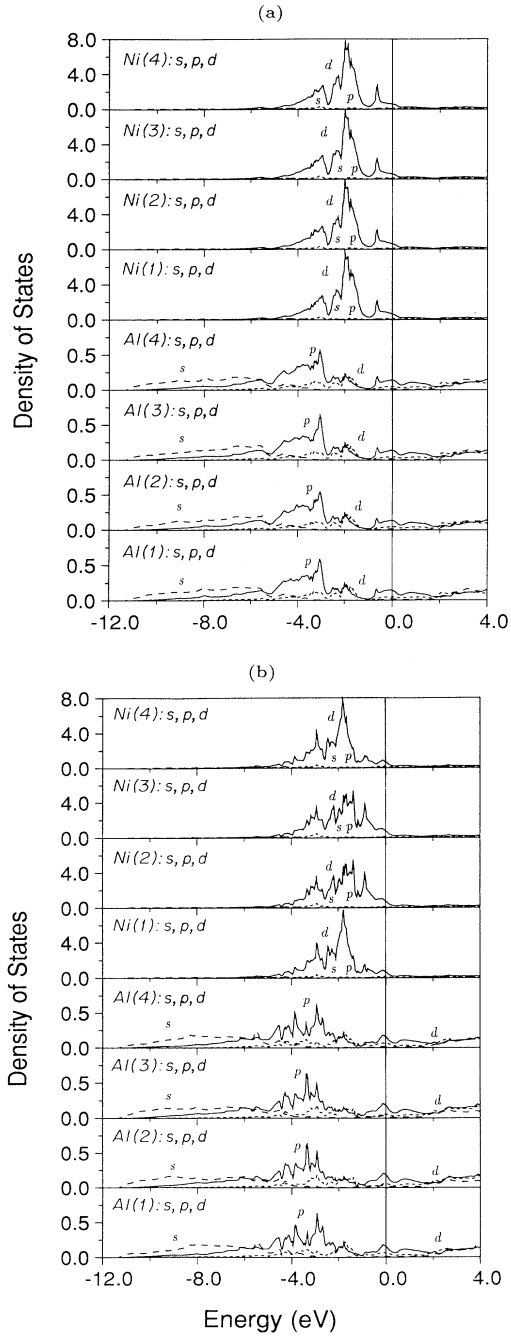

FIG. 3. Partial density of states of NiAl decomposed by atom site and angular momentum for (a) $B2$ and (b) $B2$ with APB's (in states/eV atom).

tween neighboring d electrons of Ni is dominant. By contrast, as shown in Table II, there are no first-nearest-neighbor Ni-Ni interactions available for (i) all the Ni sites in the $B2$ NiAl case and (ii) the Ni(1) and Ni(4) sites in the $B2$ with APB case. Now, since only part of the first nearest neighbors for Ni(2) and Ni(3) sites are Ni atoms, the Ni(2) and Ni(3) sites face an intermediate situation between that for $B2$ NiAl and hypothetical NiNi. Moreover, the increased width of the d bands and the enhanced partial DOS at the higher-energy side of the main peak clearly demonstrated the correlation between local environment and electronic behavior. This analysis strongly supports similar results from earlier molecular cluster calculations[34,39] (discussed above) and the tight-binding approach of Colinet *et al.*[38] in which they showed the importance of the local environment by comparing the DOS of ordered and disordered $B2$ NiAl. Now it is not difficult to see how the "pseudogap" disappears, which can be directly attributed to the d-band broadening of the Ni(2) and Ni(3) sites due to the existence of the first-nearest-neighbor Ni-Ni interactions; in turn, it indicates significant changes in bonding upon the inclusion of APB's in $B2$ NiAl.

In Table III, the partial DOS at each site and the total DOS (in states/eV atom) at E_F, and the number of electrons at each individual site and by angular momentum obtained from our $B2$ and $B2$ with APB calculations are listed. Our calculated total DOS at E_F for $B2$ and $B2$ with APB NiAl are compared with other theoretical calculations[36,37] and a low-temperature specific-heat measurement[52] for $B2$ NiAl. Among the three theoretical calculations, our calculated value for $B2$ NiAl shows the best agreement with experiment. The total DOS of $B2$ with APB is higher than that of $B2$ NiAl, which is mainly due to the d-band broadening mentioned earlier. Our calculated number of electrons for $B2$ decomposed by each site and angular momentum component shows very good agreement with the calculations of Hackenbracht and Kübler[36] done by the ASW method, which is very similar to the LMTO approach that we use. Our values are in general slightly larger than theirs: the sum of electrons at all sites and angular momentum components in their work is 0.1 electrons less than the total valence electrons in the unit cell (which they did not discuss). We should stress, however, that the number of electrons ascribed to each site is more meaningful for making comparison than are their absolute values due to the use of overlapping atomic sphere approximation (ASA) in both the LMTO and ASW methods and the indecisive division into individual atomic sites of unit cell.

The number of electrons from the $B2$ with APB calculations are little changed from the normal $B2$ NiAl for the Al(1), Al(4), Ni(1), and Ni(4) sites which have the same first and second nearest neighbors as those in normal $B2$ NiAl. For the remaining sites, the changes are mainly in the relatively mobile s and p electrons due to the changed first and second nearest neighbors, which could be accounted for by simple electronegativity considerations.

C. Comparison of charge densities and bonding

In the preceding paragraphs, we have discussed the effects of the APB's on the electronic band structures. These effects can also be demonstrated by examining the charge densities directly. Now, as the atomic sphere approximation applied in the LMTO method is unsuitable to describe the interstitial charge density, the special scheme of Christensen[53] is employed.[54] This scheme can be considered as a first-order approximation to the description of the self-consistent charge density since it utilizes the charge (or potential) obtained from the LMTO calculation only after self-consistency is reached. Therefore, the charge density shown here is qualitatively correct; note that good agreement with more precise full-potential linear augmented-plane-wave (FLAPW) results was found in previous calculations.[53,54]

The charge density on the $(1\bar{1}0)$ plane is plotted in Figs. 4(a) and 4(b) for $B2$ and $B2$ with APB NiAl. As can be seen in Fig. 4(a), the Ni atom inside the frame has four first-nearest-neighbor Al atoms on the plane. Since the two Al atoms along the horizontal axis of the figure are second nearest neighbors, this plot gives a bonding picture for both the first- and second-nearest-neighbor interactions; the second-nearest-neighbor Ni—Ni bonds are

TABLE III. Total and partial DOS at E_F (N and N_s, N_p, and N_d, respectively, in states/eV atom) along with total and angular momentum decomposed valence electrons (n and n_s, n_p and n_d) for $B2$ NiAl (with and without APB's). Except where otherwise noted, all the values listed as *other work* are from Hackenbracht and Kübler (Ref. 36).

	$B2$ NiAl with APB's				$B2$ NiAl		Other work for $B2$ NiAl	
	Al(1), Al(4)	Al(2), Al(3)	Ni(1), Ni(4)	Ni(2), Ni(3)	Al	Ni	Al	Ni
N_s	0.013	0.030	0.043	0.049	0.018	0.042	0.018	0.035
N_p	0.160	0.182	0.185	0.124	0.140	0.144	0.115	0.109
N_d	0.063	0.057	0.694	0.752	0.048	0.603	0.034	0.369
N		0.590			0.496		0.341, 0.559,[a] 0.267[b]	
n_s	0.89	0.91	0.68	0.66	0.88	0.69	0.88	0.67
n_p	1.31	1.35	0.90	0.87	1.32	0.88	1.29	0.85
n_d	0.38	0.37	8.85	8.83	0.38	8.86	0.36	8.85
n	2.58	2.63	10.43	10.36	2.58	10.42	2.53	10.37

[a]Reference 52.
[b]Reference 37.

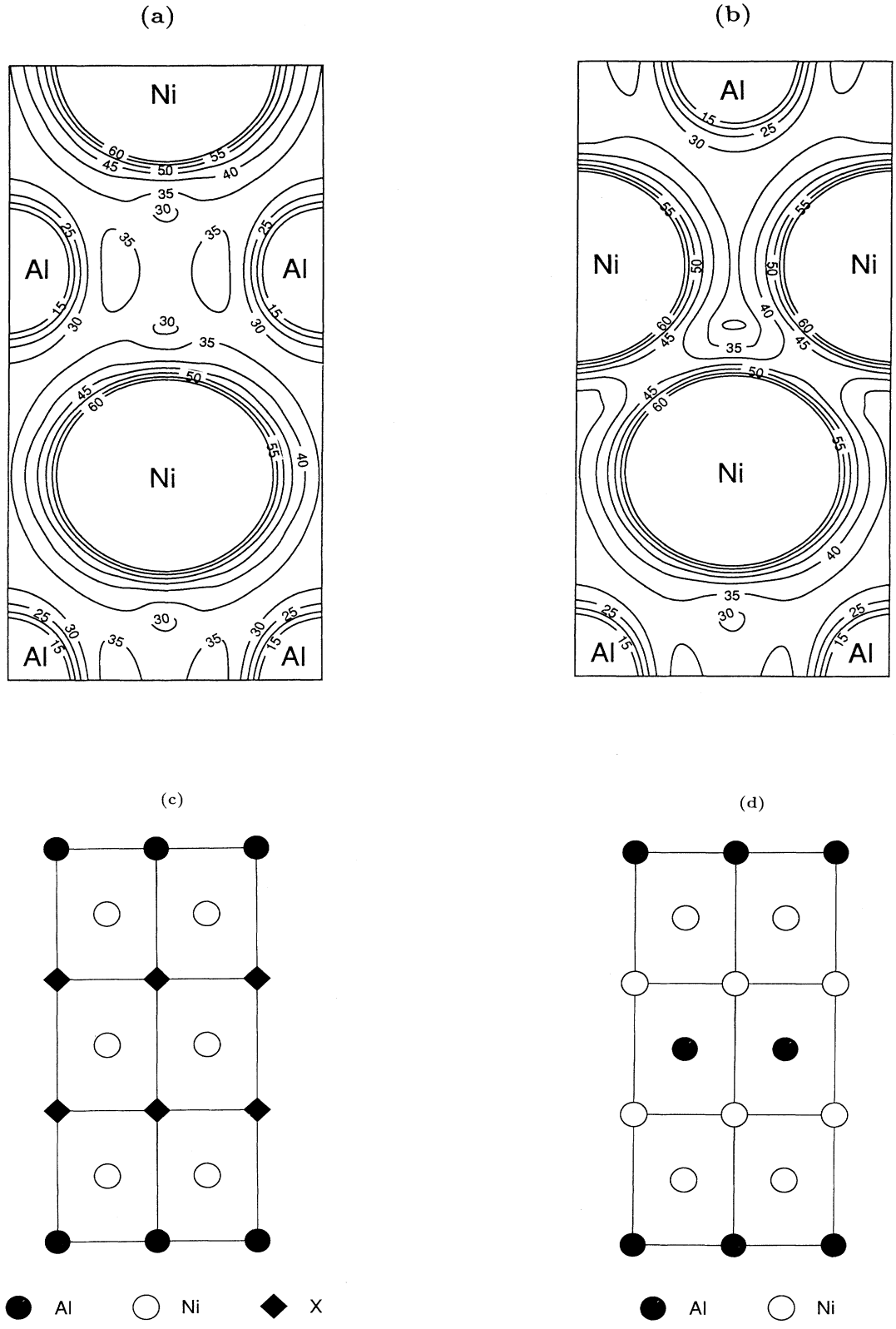

FIG. 4. Total charge density on the $(1\bar{1}0)$ plane of NiAl for (a) $B2$ and (b) $B2$ with APB's; the atomic positions on the $(1\bar{1}0)$ plane of $Ni_6Al_4X_2$ for (c) $B2$ and (d) $B2$ with APB's.

those between a Ni atom shown in the figure and two Ni atoms along the horizontal line in the two neighboring frames. To best illustrate these bonds, part of the $(1\bar{1}0)$ plane for $B2$ and $B2$ with APB-like $Ni_6Al_4X_2$ which corresponds to the region of two neighboring supercells is shown in Figs. 4(c) and 4(d). For pure NiAl, the X sites are occupied by Al atoms, as mentioned before.

It is clearly seen that there is some charge pileup along the lines connecting the first and second nearest neighbors. The large values in the region between the second-nearest-neighbor Al atoms are primarily due to the Ni atoms on the neighboring $(1\bar{1}0)$ planes right below and above the one shown here which are the first nearest neighbors to the Al atoms concerned. Cooper[55] studied electron distributions in NiAl by x-ray analysis. Since his results showed a limited charge pileup between neighboring atoms and some degree of ionicity of the bonding, the results of our first-principles calculations coincide with his description.

For $B2$ NiAl with APB [Fig. 4(b)], the charge density between Al atoms of the first row (counted from the bottom horizontal line) which represents the second-nearest-neighbor Al-Al interaction, and that between those Al atoms and Ni atom of the second row (the first-nearest-neighbor Ni-Al interaction) change little from the $B2$ case. So does the charge density between Ni atoms of the second (as well as third) row [cf., Fig. 4(d)] which represents the second-nearest-neighbor Ni-Ni interaction. However, those first-nearest-neighbor Ni-Al interactions between the second and third row atoms in the $B2$ case are now replaced by the first-nearest-neighbor Ni-Ni interactions [or Al-Al interactions on the neighboring $(1\bar{1}0)$ planes, whose charge density is not shown here because of space considerations]. There is a moderate charge pileup along lines connecting these first-nearest-neighbor Ni atoms. Once again, the importance of the first nearest neighbors (or rather, the local environment) is demonstrated unambigiously.

From our calculations and other earlier work, strong Ni d and Al p interactions in $B2$ NiAl are well established. The existence of the "pseudogap" which separates the antibonding from bonding and nonbonding regions is an obvious indication of that strong interaction. By filling up the "pseudogap" in the case of $B2$ NiAl with APB's, the clear separation of antibonding from bonding and nonbonding states is no longer seen. Hence, the strong interaction in $B2$ NiAl is significantly modified (weakened) by the creation of APB's which means the formation of APB's in $B2$ NiAl is energetically unfavorable.

Following this analysis, we may speculate further as to which elements are potentially likely to decrease the APB energies, i.e., to promote $\langle 111 \rangle$ slip in $B2$ NiAl. As the creation of APB's ($\langle 111 \rangle$ type) inevitably changes the local environment (the first nearest neighbors), good candidates may be those for which the modification of the local environment accompanying the creation of APB's would not produce changes in electronic and other behavior as enormous as those in pure $B2$ NiAl. In other words, we need some intermediate elements which do not interact with Al (Ni) as strongly as Ni (Al). It is well known that the d bands would shift downward in energy with increasing atomic number for transition elements of the same row,[56] and that the interaction between bands depends strongly on their overlap in energy. Hence, the earlier transition metals with their d bands lying higher in energy than Ni may fulfill such needs. In Sec. IV, we discuss the results of our APB calculations for $B2$ NiAl with ternary additions Cr and V substituting for either Ni or Al as well as Mn substituting for Ni.

IV. RESULTS FOR NiAl WITH SELECTED TERNARY ADDITIONS

A. APB energies

For computational efficiency and to avoid the extreme four-layer APB case in which the upper and low APB interfaces are on the same plane, we select six-layer cells for calculations with ternary additions. Since the calculated APB energies in the $\frac{1}{2}\langle 111 \rangle$ on $\{112\}$ case were shown to have the same trend as those for $\frac{1}{2}\langle 111 \rangle$ on $\{110\}$ in pure NiAl, we expect the same situation to happen for NiAl with ternary additions. Therefore, we concentrate our calculations on the $\frac{1}{2}\langle 111 \rangle$ on $\{110\}$ APB only. In order to have the maximum effect on the APB interface, the ternary additions replace either Ni or Al in the two APB interface planes.

The calculated APB energy values are listed in Table IV, along with the formation energies of these hypothetical $B2$ compounds which are obtained by taking the difference of total energy of each hypothetical compound and the sum of their constituent metals in their states of lowest total energy (except Mn, for which we take the total energy of the paramagnetic fcc lattice, rather of its complex antiferromagnetic structure). The total energies of individual ternary elements were obtained in a related LMTO study by Lin and Freeman.[57] The absolute values in Table IV should not be taken too seriously since the APB energies would decrease as the number of layers between two consecutive APB's increases (as shown in Table I).

It is surprising that the APB energies are only a quarter of the value of pure $B2$ NiAl if the ternary V and Cr were to substitute Ni and Al, respectively. Unfortunately, these specific site occupancies are exactly those which are energetically unfavored—as can be seen by comparing the formation energies for these hypothetical com-

TABLE IV. APB energies (in mJ/m^2) of $B2$ NiAl with ternary additions and the formation energies (in mRy/atom) for the compounds with a $B2$-like cell.

Composition	APB energy	Formation energy
Ni_6Al_6	1000	−43.5
$Ni_6Al_4V_2$	550	−25.2
$Ni_4Al_6V_2$	250	+3.4
$Ni_6Al_4Cr_2$	250	−16.1
$Ni_4Al_6Cr_2$	510	−25.7
$Ni_4Al_6Mn_2$	740	−41.3

pounds. Therefore, the most dramatic cases of lowering APB energies are partly attributable to the relatively less stable nature of those compositions in the $B2$-like structure. Nevertheless, reduction of APB energies to as much as one-half may be obtained with the addition of the ternary elements V and Cr. The case of substituting Mn for Ni turns out to give a less decreased APB energy than do the other additions and a comparable formation energy with pure NiAl (which may be partly caused by using results of paramagnetic fcc Mn rather than the observed state in getting the formation energy, as mentioned above). From all these data, a correlation between high formation energy and high APB energy can be found which perhaps makes the formation energy a rough measure of the APB energy.

As mentioned earlier, the APB energies in Ni_3Al were calculated to be much lower than in NiAl. However, APB's are not always seen, even in Ni_3Al.[22,58–61] Although the APB energies of NiAl with ternary additions of Cr and V are lowered significantly from those in pure NiAl, they are still much larger than the values in Ni_3Al. If we take the APB energy of Ni_3Al as a rough measure for APB's to occur, it remains difficult to activate APB's in these modified NiAl systems caused by the extremely high APB energies in pure NiAl. Based on our preliminary results that ternary additions V and Cr would dramatically lower the antiphase boundary energies in $B2$ NiAl,[29] Darolia *et al.*[30,31] have tried to add V and Cr to $B2$ NiAl and ⟨111⟩ slip is still missing from their results. At this point, it is not difficult to explain the results of Miracle *et al.*[14] and Darolia *et al.*[30,31] Note that these model calculations were designed to maximize the effect of ternary additions on the APB energy by putting the ternary additions onto the APB interfacial planes, and hence, since the ternary additions do not necessarily segregate to APB interface planes, the results should be considered as an upper limit. However, when this overestimation is combined with the approximation of no relaxation, these results should perhaps be more meaningful than those for the pure NiAl case because the two approximations have the opposite effect.

In the following, we take a close look at the effect of

TABLE V. The first- and second-nearest-neighbor (NN) configurations for $B2$- and $B2$ with APB-like cells (labeled as $B2$ and APB, respectively) for $Ni_6Al_4V_2$ and $NI_4Al_6V_2$.

		1st NN			2nd NN		
$Ni_6Al_4V_2$		Ni	Al	V	Ni	Al	V
$B2$	Al(1)	8	0	0	0	6	0
	Al(2)	8	0	0	0	4	2
	V	8	0	0	0	4	2
	Al(4)	8	0	0	0	2	4
	Ni(1)	0	8	0	6	0	0
	Ni(2)	0	6	2	6	0	0
	Ni(3)	0	4	4	6	0	0
	Ni(4)	0	4	4	6	0	0
APB	Al(1)	8	0	0	0	6	0
	Al(2)	6	0	2	2	4	0
	V	6	2	0	2	2	2
	Al(4)	8	0	0	0	2	4
	Ni(1)	0	8	0	6	0	0
	Ni(2)	2	6	0	4	0	2
	Ni(3)	2	2	4	4	2	0
	Ni(4)	0	4	4	6	0	0
$B2$	Al(1)	8	0	0	0	6	0
	Al(2)	6	0	2	0	6	0
	Al(3)	4	0	4	0	6	0
	Al(4)	4	0	4	0	6	0
	Ni(1)	0	8	0	6	0	0
	Ni(2)	0	8	0	4	0	2
	V	0	8	0	4	0	2
	Ni(4)	0	8	0	2	0	4
APB	Al(1)	8	0	0	0	6	0
	Al(2)	6	2	0	0	4	2
	Al(3)	2	2	4	2	4	0
	Al(4)	4	0	4	0	6	0
	Ni(1)	0	8	0	6	0	0
	Ni(2)	0	6	2	4	2	0
	V	2	6	0	2	2	2
	Ni(4)	0	8	0	2	0	4

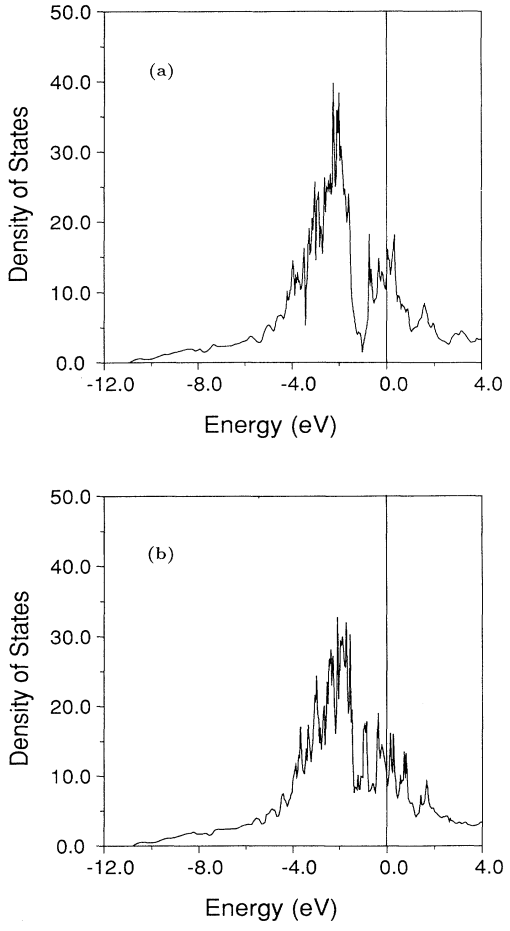

FIG. 5. Total density of states of $Ni_6Al_4V_2$ for (a) $B2$-like and (b) $B2$ with APB-like cells (in states/eV unit cell).

ternary additions on the electronic and bonding properties of the modified systems. Since the ternary additions selected are neighboring elements in the $3d$ row, we believe that they would behave more or less similarly, so we take V as an example to shed some light on the behavior of the modified NiAl systems. In Table V, the first and second nearest neighbors of $Ni_6Al_4V_2$ (V substituting Al) and $Ni_4Al_6V_2$ (V substituting Ni) in $B2$-like and $B2$ with APB-like cells are listed. For convenience, we keep the same notation as in pure NiAl for all the sites except for those substituted by the ternary V atoms, i.e., there are no Al(3) [Ni(3)] sites in $Ni_6Al_4V_2$ ($Ni_4Al_6V_2$).

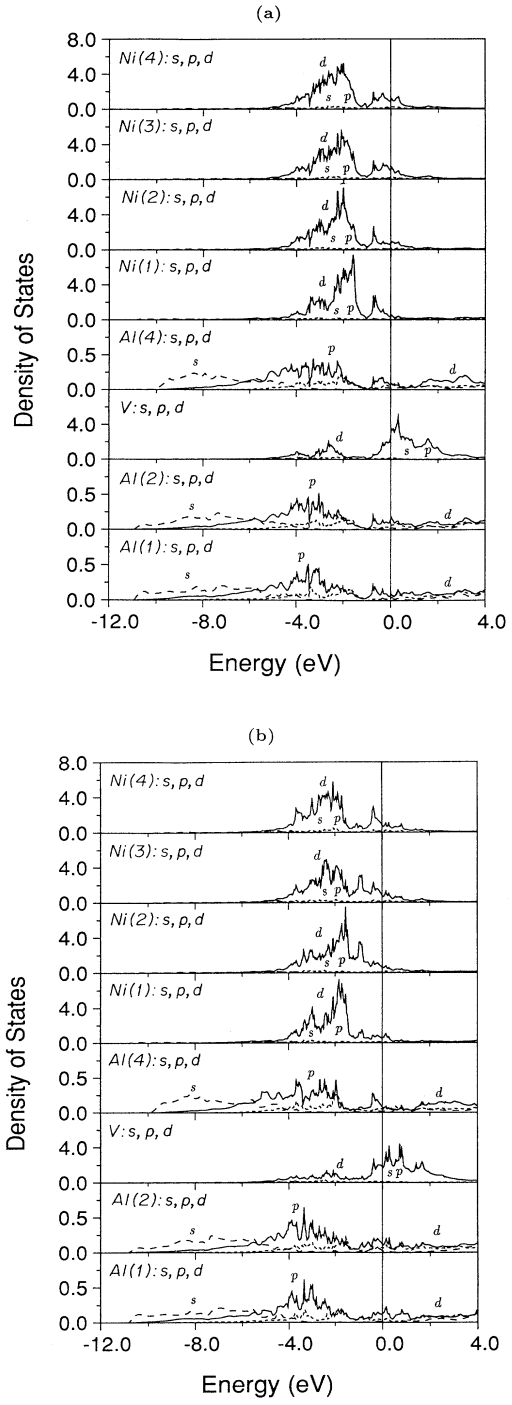

FIG. 6. Partial density of states of $Ni_6Al_4V_2$ decomposed by atom site and angular momentum for (a) $B2$-like and (b) $B2$ with APB-like cells (in states/eV atom).

B. Comparison of densities of states

The total and partial DOS at each site for $B2$- and $B2$ with APB-like $Ni_6Al_4V_2$ and $Ni_4Al_6V_2$ are plotted in Figs. 5–8, respectively. By comparing these plots with those for the pure NiAl calculations (Figs. 2 and 3), some interesting points can be noted immediately. To a large extent, the plots for $Ni_6Al_4V_2$ have the same character as those for pure NiAl. A "pseudogap" occurs in the $B2$-like case and it disappears in $B2$ with the APB-like one. For those Ni sites that have the same first and second nearest neighbors as the Ni atoms in pure NiAl the plots look much the same, which emphasizes the importance of the local environment as shown repeatedly above. Perhaps the most significant change in this modified system is the broadening of the antibonding side of the d-p hybridized bands for those Ni sites which have some V atoms (substituting Al) as their first nearest neighbors.

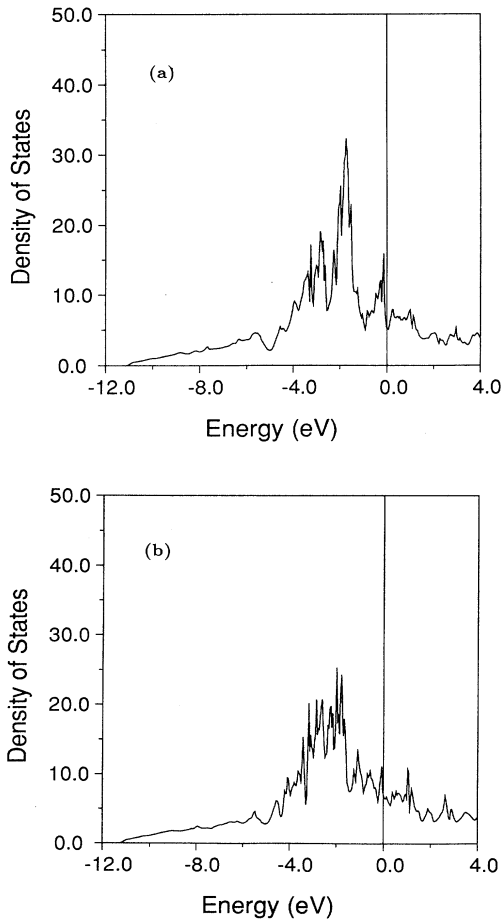

FIG. 7. Total density of states of $Ni_4Al_6V_2$ for (a) $B2$-like and (b) $B2$ with APB-like cells (in states/eV unit cell).

This can be directly associated with the character of the V d bands which are higher in energy, and may also explain why the smaller difference in total bonding between the $B2$- and $B2$ with APB-like cells (or, smaller APB energy) occurs in $Ni_6Al_4V_2$ rather than in pure NiAl, as we argued above in selecting potential ternary additions.

In contrast with the $Ni_6Al_4V_2$ case, the plots for

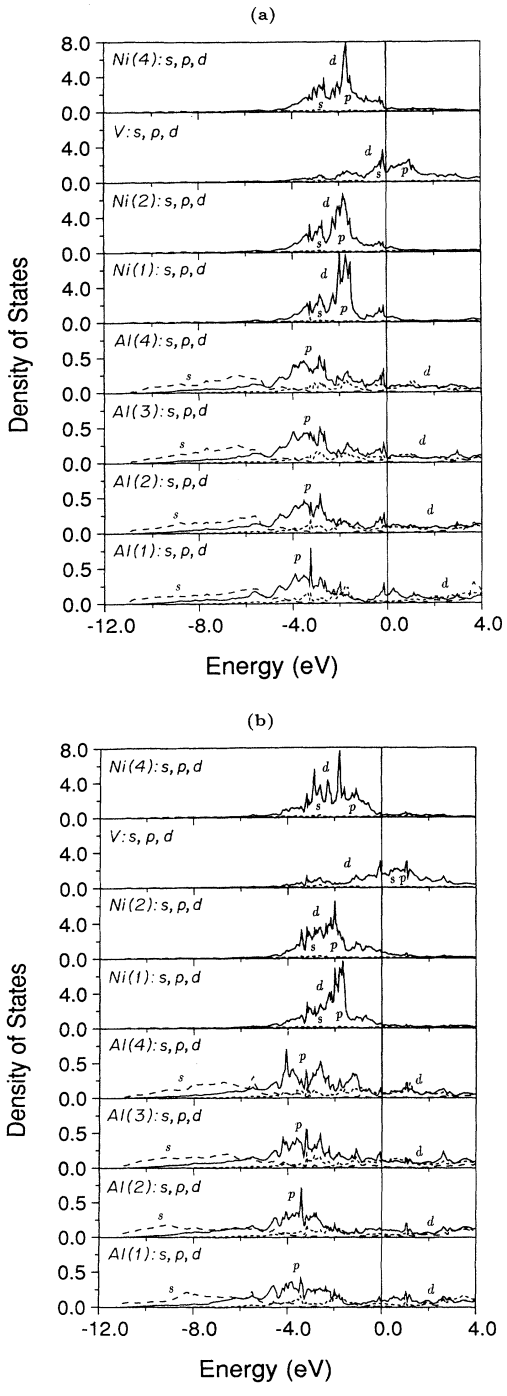

FIG. 8. Partial density of states of $Ni_4Al_6V_2$ decomposed by atom site and angular momentum for (a) $B2$-like and (b) $B2$ with APB-like cells (in states/eV atom).

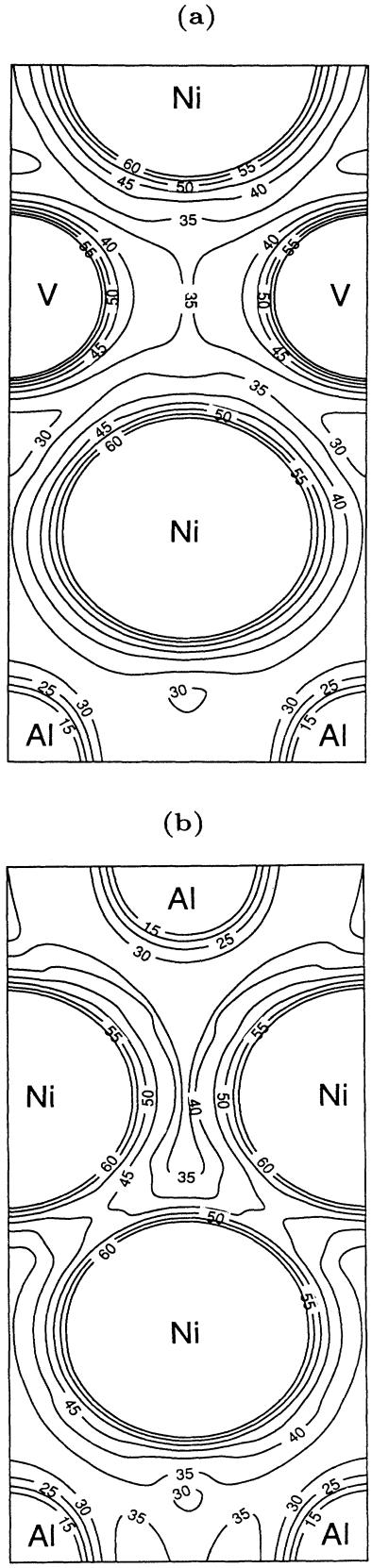

FIG. 9. Total charge density on the $(1\bar{1}0)$ plane of $Ni_6Al_4V_2$ for (a) $B2$-like and (b) $B2$ with APB-like cells.

TABLE VI. Number of electrons by atomic site and angular momentum for $Ni_6Al_4V_2$ in $B2$- and $B2$ with APB-like cells.

	$B2$				APB			
	n_s	n_p	n_d	n	n_s	n_p	n_d	n
Al(1)	0.89	1.31	0.37	2.57	0.89	1.31	0.38	2.58
Al(2)	0.89	1.32	0.38	2.58	0.95	1.36	0.37	2.68
V	0.50	0.66	3.37	4.53	0.50	0.66	3.45	4.61
Al(4)	0.89	1.33	0.38	2.59	0.89	1.33	0.37	2.59
Ni(1)	0.69	0.86	8.88	10.42	0.68	0.88	8.83	10.40
Ni(2)	0.73	0.90	8.80	10.43	0.68	0.86	8.80	10.34
Ni(3)	0.75	0.92	8.78	10.44	0.74	0.90	8.74	10.38
Ni(4)	0.77	0.92	8.75	10.44	0.76	0.92	8.75	10.43

$Ni_4Al_6V_2$ (Figs. 7 and 8) show drastic changes from those for pure NiAl. The "pseudogap" disappears even in the $B2$-like case and is replaced by a valley with a moderate value at the bottom. It is now no longer feasible to define the bonding, nonbonding and antibonding regions. The differences between the $B2$ and $B2$ with APB-like cases are not as obvious as those discussed earlier. The lack of the "pseudogap" may explain the unstable nature of this composition in the $B2$-like case since it indicates that there is not a strong enough interaction to split the bonding and antibonding states.

For comparison, the number of electrons at each site and by angular momentum for $Ni_6Al_4V_2$ ($B2$- and $B2$ with APB-like) and $Ni_4Al_6V_2$ ($B2$- and $B2$ with APB-like) cases are listed in Tables VI and VII, respectively. Again, these numbers are more meaningful for comparisons due to the approximation of using overlapping atomic spheres and equal sphere sizes. As shown in the discussion of the DOS plots for $Ni_6Al_4V_2$, the change of values accompanying the creation of APB's is very similar to that for pure NiAl. Although the number of total valence electrons at Ni and Al sites is about the same in $Ni_6Al_4V_2$ and NiAl with $B2$-like cells, the number of d electrons at those Ni sites in $Ni_6Al_4V_2$ which have V as part of the first nearest neighbors is about 0.1 less than those Ni sites of pure NiAl. This can be attributed to the existence of Ni d and V d interactions which are expected to shift the center of Ni d bands upward. Consequently, the filled portion of the Ni d bands is decreased. By looking at the number of electrons for $Ni_4Al_6V_2$ (cf., Table VII), it is easily found that these values are changed significantly from the pure NiAl case, as are the DOS plots discussed above. This large change reflects the large modification of the bonding which is found to be unfavorable as in earlier discussions of the formation energies.

C. Charge densities and bonding

To see how the ternary additions modify the spatial distribution of the valence electrons, we plot in Fig. 9 the charge density on the $(1\bar{1}0)$ plane of $B2$- and $B2$ with APB-like $Ni_6Al_4V_2$. In $B2$-like $Ni_6Al_4V_2$, the charge pileup between the first-nearest-neighbor Ni and V atoms is barely seen, while that between the first-nearest-neighbor Ni and Al atoms is about the same as the one in pure NiAl. The charge density between the second-nearest-neighbor Ni-Ni is also little changed, and that between the second-nearest-neighbor Al-Al is even slightly smaller. This may imply that the total bonding is weakened in $B2$-like $Ni_6Al_4V_2$ compared with $B2$ NiAl.

By contrast, the charge density between the first-nearest-neighbor Ni atoms is noticeably increased in the $B2$ with APB-like $Ni_6Al_4V_2$ compared with NiAl with APB's, while that between the first-nearest-neighbor Ni-Al is about the same for the two cases. This would give rise to an enhanced total bonding in $B2$ with APB-like $Ni_6Al_4V_2$ compared with $B2$ with APB NiAl. Combining the opposite changes of bonding in $B2$- and $B2$ with

TABLE VII. Number of electrons at each atomic site and by angular momentum for $Ni_4Al_6V_2$ in $B2$- and $B2$ with APB-like cells.

	$B2$				APB			
	n_s	n_p	n_d	n	n_s	n_p	n_d	n
A(1)	0.88	1.30	0.37	2.56	0.89	1.28	0.37	2.54
Al(2)	0.93	1.39	0.39	2.71	0.91	1.37	0.39	2.67
Al(3)	0.96	1.47	0.40	2.83	0.99	1.50	0.40	2.90
Al(4)	0.96	1.46	0.40	2.82	0.96	1.45	0.41	2.82
Ni(1)	0.67	0.85	8.85	10.37	0.68	0.88	8.85	10.40
Ni(2)	0.70	0.89	8.84	10.43	0.73	0.93	8.81	10.47
V	0.49	0.70	3.76	4.94	0.49	0.70	3.68	4.87
Ni(4)	0.71	0.90	8.83	10.43	0.71	0.90	8.84	10.44

APB-like $Ni_6Al_4V_2$ from $B2$ and $B2$ with APB NiAl, respectively, the decrease of APB energy in $Ni_6Al_4V_2$ can be explained. For the charge density of $Ni_4Al_6V_2$ in $B2$- and $B2$ with APB-like cells, the large changes from those of NiAl make it hard to compare these two cases.

V. SUMMARY

Our calculated APB energies for pure NiAl are extremely high, while those for NiAl with ternary additions of V and Cr are significantly reduced (in other words, the formation of APB in the region where the ternary additions are located is significantly eased). However, the reduction is probably not large enough to activate ⟨111⟩ slip if we take the APB energies of Ni_3Al as a crude measure for the APB activation energy required in NiAl. Our results imply that it is a tough task to achieve ⟨111⟩ slip in NiAl by promoting the APB's as this requires a reduction of the APB energy of the order of 70–80%, which serves as a conservative estimate. The origin of the high APB energy is related to the first-nearest-neighbor changes with the inclusion of APB in $B2$ NiAl. This and other electronic properties may be helpful in guiding future alloying efforts.

ACKNOWLEDGMENTS

We thank W. Lin for providing the data (mentioned in the text) from a related study and the charge-density construction program. Helpful discussions and collaboration with R. Darolia, D. M. Dimiduk, R. D. Field, and D. B. Miracle were very valuable to this study and are gratefully acknowledged. We thank C. L. Fu for critical comments on this paper. This work was supported by the Air Force Office of Scientific Research (Grant No. 88-0346 and under Contract No. F49620-88-C-0052), by the Department of Energy, and by a computing grant from Basic Energy Sciences, Department of Energy at the NERSC, Lawrence Livermore National Laboratory.

[1]R. L. Fleischer, D. M. Dimiduk, and H. A. Lipsitt, Annu. Rev. Mater. Sci. **19**, 231 (1989).

[2]James L. Smialek and Robert F. Hehemann, Metall. Trans. **4**, 1571 (1973).

[3]Norman S. Stoloff, in *High-Temperature Intermetallic Ordered Alloys,* Materials Reserach Society Symposium Proceedings, edited by C. C. Koch, C. T. Liu, and N. S. Stoloff (Materials Research Society, Pittsburgh, 1985), Vol. 39, p. 3.

[4]K. Vedula and J. R. Stephens, in *High-Temperature Intermetallic Ordered Alloys II,* Materials Research Society Symposium Proceedings, edited by N. S. Stoloff, C. C. Koch, C. T. Liu, and O. Izumi (Materials Research Society, Pittsburgh, 1987), Vol. 81, p. 381.

[5]J. R. Stephens, in *High-Temperature Intermetallic Ordered Alloys* (Ref. 3), p. 381.

[6]J. R. Stephens and M. V. Nathal, in *Superalloys 1988,* edited by S. Reichman, D. N. Duhl, G. Maurer, S. Antolovich, and C. Lund (The Metallurgical Society, Warrendale, PA, 1988), p. 183.

[7]I. Baker, in *High Temperature Aluminides and Intermetallics,* edited by S. H. Whang, C. T. Liu, and D. Pope (Metallurgical Society of the American Institute of Mechanical Engineers, Warrendale, PA, 1989).

[8]D. L. Anton, D. M. Shah, D. N. Duhl, and A. F. Giamei, J. Met. **41**, 12 (1989).

[9]O. Kubaschewski, Trans. Faraday Soc. **54**, 814 (1958).

[10]See, for example, J. H. Westbrook, H. E. Grenoble, and W. L. Wood, Technical Report No. WADD-TR-60-194, Part 5, March, 1964 (unpublished); R. T. Pascoe and C. W. A. Newey, Phys. Status Solidi **29**, 357 (1968); Met. Sci. J. **2**, 138 (1968); M. H. Loretto and R. J. Wasilewski, Philos. Mag. **23**, 1311 (1971).

[11]A. Ball and R. E. Smallman, Acta Metall. **14**, 1517 (1966); **16**, 233 (1968).

[12]R. J. Wasilewski, S. R. Butler, and J. E. Hanlon, Trans. Metall. Soc. AIME **239**, 1357 (1967).

[13]H. L. Fraser, R. E. Smallman, and M. H. Loretto, Philos. Mag. **28**, 651 (1973); **28**, 667 (1973); C. H. Lloyd and M. H. Loretto, Phys. Status Solidi **39**, 163 (1970).

[14]D. B. Miracle, S. Russell, and C. C. Law, in *High-Temperature Intermetallic Ordered Alloys III,* Materials Research Society Symposium Proceedings, edited by C. T. Liu, A. I. Taub, N. S. Stoloff, and C. C. Koch (Materials Research Society, Pittsburgh, 1989), Vol. 133, p. 225.

[15]S. M. Copley, Philos. Mag. **8**, 1599 (1963).

[16]R. von Mises, Z. Angew. Math. Mech. **8**, 161 (1928).

[17]See, for example, A. Ball and R. E. Smallman, Acta Metall. **14**, 1349 (1966).

[18]A. G. Rozner and R. J. Wasilewski, J. Inst. Met. **94**, 169 (1966).

[19]K. Vedula, K. H. Hahn, and B. Boulogne, in *High-Temperature Intermetallic Ordered Alloys III* (Ref. 14), p. 229; K. H. Hahn and K. Vedula, Scr. Metall. **23**, 7 (1989).

[20]E. M. Schulson and D. R. Barker, Scr. Metall. **17**, 519 (1983); E. M. Schulson, in *High-Temperature Ordered Intermetallic Alloys* (Ref. 3), p. 193.

[21]D. J. Gaydosh, R. W. Jech, and R. H. Titron, J. Mater. Sci. Lett. **4**, 138 (1985).

[22]C. C. Koch, in *High-Temperature Ordered Intermetallic Alloys* (Ref. 3), p. 397.

[23]A. I. Taub and M. R. Jackson, in *Rapidly Solidified Alloys and Their Mechanical and Magnetic Properties,* Materials Research Society Symposium Proceedings, edited by B. C. Giessen, D. E. Polk, and A. I. Taub (Materials Research Society, Pittsburgh, 1986), Vol. 58, p. 389.

[24]E. M. Schulson, *COSAM Program Overview,* NASA TN 830006 (unpublished).

[25]R. D. Noebe and R. Gibala, in *High-Temperature Ordered Intermetallic Alloys* (Ref. 3), p. 319; R. Gibala, R. D. Noebe, J.-T. Kim, and M. Larsen, in *High-Temperature Aluminides and Intermetallics* (Ref. 7).

[26]W. A. Rachinger and A. H. Cottrell, Acta Metall. **4**, 109 (1956).

[27]V. B. Kurfman, Acta Metall. **13**, 307 (1965).

[28]D. I. Potter, Mater. Sci. Eng. **5**, 201 (1969/1970).

[29]Preliminary results were presented previously, cf., T. Hong and A. J. Freeman, in *High-Temperature Intermetallic Ordered Alloys III* (Ref. 14), p. 75.

[30]R. Darolia, D. F. Lahrman, R. D. Field, and A. J. Freeman, in *High-Temperature Intermetallic Ordered Alloys III* (Ref. 14), p. 113.
[31]R. Darolia, R. D. Field, D. F. Lahrman, and A. J. Freeman, in *High Temperature Aluminides and Intermetallics* (Ref. 25).
[32]J. W. D. Connolly and K. H. Johnson, in *Electron Density States,* Natl. Bur. Stand. (U.S.) Spec. Publ. No. 323, edited by L. H. Bennett (U.S. GPO, Washington, D.C., 1971), p. 151.
[33]V. L. Moruzzi, A. R. Williams, and J. F. Janak, Phys. Rev. B **10**, 4856 (1974).
[34]D. E. Ellis, G. A. Benesh, and E. Byrom, Phys. Rev. B **20**, 1198 (1979).
[35]Ch. Müller, H. Wonn, W. Blau, P. Zieshe, and V. P. Krivitskii, Phys. Status Solidi B **95**, 215 (1979).
[36]D. Hackenbracht and J. Kübler, J. Phys. F **10**, 427 (1980).
[37]R. Eibler and A. Neckel, J. Phys. F **10**, 2179 (1980).
[38]C. Colinet, B. Bessoud, and A. Pasturel, J. Phys. Condens. Matter **1**, 5837 (1989).
[39]D. D. Sarma, W. Speier, R. Zeller, E. Van Leuken, R. A. de Groot, and J. C. Fuggle, J. Phys. Condens. Matter **1**, 9131 (1989).
[40]O. K. Andersen, Phys. Rev. B **12**, 3060 (1975); T. Oguchi and A. J. Freeman, J. Magn. Magn. Mater. **46**, L1 (1984).
[41]T. Hong, T. J. Watson-Yang, A. J. Freeman, T. Oguchi, and J.-H. Xu, Phys. Rev. B **41**, 12 462 (1990).
[42]T. Hong, T. J. Watson-Yang, X-Q. Guo, A. J. Freeman, J.-H. Xu, and T. Oguchi, Phys. Rev. B **43**, 1940 (1991).
[43]P. Villars and L. D. Calvert, *Pearson's Handbook of Crystallographic Data for Intermetallic Phases* (American Society for Metals, Metals Park, OH, 1985), Vol. 2, p. 1038.
[44]J. Xu and A. J. Freeman (unpublished); C. L. Fu and A. J. Freeman (unpublished).
[45]L. A. Girifalco and J. A. Alonso, in *Theory of Alloy Phase Formation,* edited by L. H. Bennett (Metallurgical Society of the American Institute of Mechanical Engineers, Warrendale, PA, 1980), p. 218.
[46]M. Rudy and G. Sauthoff, in *High-Temperature Ordered Intermetallic Alloys* (Ref. 3), p. 327.
[47]C. L. Fu, J. Mater. Res. **5**, 971 (1990).
[48]S. M. Foiles and M. S. Daw, J. Mater. Res. **2**, 5 (1987).
[49]S. P. Kowalczyk, G. Apai, G. Kaindl, F. McFeely, L. Ley, and D. A. Shirley, Solid State Commun. **25**, 847 (1978); P. T. Andrews, T. Collins, and P. Weightman, J. Phys. C **15**, L3557 (1981).
[50]J. C. Fuggle, F. Ulrich Hillebrecht, R. Zeller, Zygmunt Zolnierek, and Peter A. Bennett, Phys. Rev B **27**, 2145 (1983) and references therein.
[51]P. O. Nilsson, Phys. Status Solidi **41**, 317 (1970).
[52]J. J. Begot, R. Caudron, P. Faivre, A. Lasalmonie, and P. Costa, J. Phys. (Paris) Lett. **35**, L225 (1974).
[53]N. E. Christensen, Phys. Rev. B **29**, 5547 (1984).
[54]The program used is implemented independently in our group. See W. Lin and A. J. Freeman (unpublished).
[55]M. J. Cooper, Philos. Mag. **89**, 811 (1963).
[56]See, for example, D. G. Pettifor, in *Physical Metallurgy,* edited by R. W. Cahn and P. Haasen (North-Holland, Amsterdam, 1983), Chap. 3.
[57]W. Lin and A. J. Freeman (unpublished).
[58]A. Korner, Philos. Mag. A **58**, 507 (1988).
[59]Y. Q. Sun and P. M. Hazzledine, Philos. Mag. A **58**, 603 (1988).
[60]M. J. Mills, N. Baluc, and H. P. Karthaler, in *High-Temperature Intermetallic Ordered Alloys III* (Ref. 14).
[61]P. Veyssiere, in *High-Temperature Intermetallic Ordered Alloys II* (Ref. 14).